Hybrid Monte Carlo Simulation of Graphene on the Hexagonal Lattice

R. C. Brower,[1,2] C. Rebbi,[1,2] and D. Schaich[1,2]

[1]*Department of Physics, Boston University, 590 Commonwealth Avenue, Boston, MA 02215, United States of America*
[2]*Center for Computational Science, Boston University, 3 Cummington Street, Boston, MA 02215, United States of America*

(Dated: January 16, 2012)

The tight binding Hamiltonian for graphene on the hexagonal carbon lattice is believed to provide an accurate theoretical representation, but with no analytical solution, quantitatively precise predictions are lacking. We construct the exact field theoretic Lagrangian on the hexagonal lattice and demonstrate, for the nearest neighbor hopping terms and a long range Coulomb interaction between the electrons, that standard numerical methods for lattice field theory can be performed with no sign problem. Consequently we present a method that enables the exact tight binding solution to be found numerically to arbitrary precision on a finite hexagonal lattice, subject only to the continuum extrapolation for the discrete Euclidean time. This will allow for the first time quantitatively precise *ab initio* predictions to confront the tight binding theory with experiment.

PACS numbers: 11.15.Ha, 05.10.Ln

Introduction Graphene, a single layer of carbon atoms forming a hexagonal lattice, has remarkable experimental properties [1, 2] with vast technological potential under intensive investigation. Moreover the tight-binding Hamiltonian is believed to provide an accurate theoretical representation [3], with a low energy spectrum for the electrons equivalent to Dirac fermions for a relativistic field in two dimensions. This observation has prompted some researchers to adapt to graphene lattice gauge theory techniques [4] which have been profitably applied to the study of Quantum Chromodynamics and other relativistic particle systems. This approach [5–8] replaces the tight binding theory by the effective low energy Dirac Hamiltonian and then places the Dirac field on a staggered 4d hypercubic lattice with a static electric gauge field to induce a long range Coulomb interaction. Although this approach has led to very interesting and valuable results [5–8], all contact with the physical carbon lattice and experimentally determined lattice constants of the tight-binding model is lost. On the other hand, it should be possible to apply the hybrid Monte Carlo technique directly to the hexagonal graphene lattice. The clear advantage of this approach would be a real understanding of the dependence on microscopic details. In this letter we show how this can be done.

Graphene is a system of interacting electrons located at the vertices of a hexagonal lattice. It is convenient to think of the graphene lattice as consisting of two triangular sublattices, which we denote by A and B, which together with the centers of the hexagons (sublattice C) form a finer, underlying triangular lattice (Fig. 1). We introduce fermionic annihilation and creation operators $a_{x,s}, a^\dagger_{x,s}$ for the electrons on the two sublattices, where x is a site index and $s = \pm 1$ is the spin index. The lattice must be made finite in order to perform numerical simulations. While there is a broad range of boundary conditions of physical interest, here we consider periodic systems formed by identifying opposing sides of a hexagonal lattice of length L, illustrated in Fig. 1 for $L = 4$.

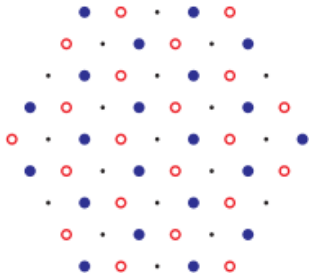

FIG. 1: The hexagonal graphene lattice consists of the two Bravais triangular sublattices A (solid) and B (empty).

The tight-binding Hamiltonian H consists of two terms. The quadratic kinetic term is

$$H_2 = \sum_{\langle x,y\rangle,s} -\kappa(a^\dagger_{x,s}a_{y,s} + \text{h.c.}), \tag{1}$$

where the sum runs over all pairs $\langle x, y\rangle$ of nearest neighbor sites (coupling the A and B sublattices) and the two values of the spin. The Coulomb interaction term is

$$H_C = \sum_{x,y} e^2 V_{x,y} q_x q_y, \tag{2}$$

where $q_x = a^\dagger_{x,1}a_{x,1} + a^\dagger_{x,-1}a_{x,-1} - 1$ is a local charge operator and V is the interaction potential. We have explicitly introduced the charge coupling constant e.

Several comments are in order. First note that in the kinetic term we have neglected the smaller next-to-nearest neighbor hopping within each sublattice, which would introduce a small (probably manageable) complex phase in the path integral. The charge operator q_x has a -1 to account for the background charge of the carbon ion: it ensures that the system is neutral at half filling,

and it will play an important role for our functional integral formulation. V could be the actual 3d Coulomb potential, but could be any other interaction potential. The only constraint is that the matrix $V_{x,y}$ must be positive definite. Finally, we note that the Hamiltonian of Eqs. 1-2 commutes with the angular momentum generators,

$$J_\pm = a^\dagger_{x,s}\sigma^{ss'}_\pm a_{x,s'}, \qquad J_3 = a^\dagger_{x,s}\sigma^{ss'}_3 a_{x,s'}/2\ , \tag{3}$$

which act on the spin of the electron and play the role in the tight-binding model of an internal or "isospin" symmetry.

In order to explore the properties of the system one would like to calculate expectation values

$$\langle \mathcal{O}_1(t_1)\mathcal{O}_2(t_2)\dots\rangle = Z^{-1}\mathrm{Tr}\, T[\mathcal{O}_1(t_1)\mathcal{O}_2(t_2)e^{-\beta H}]\ , \tag{4}$$

where β can be interpreted as an extent in Euclidean time, $T[\dots]$ stands for time ordering of the operators inside the square bracket with respect to the Euclidean evolution implemented by $\exp(-\beta H)$, and $Z = \mathrm{Tr}\,\exp(-\beta H)$ is the partition function.

Path integral form Our goal is to provide an equivalent path integral formulation of Eq. 4 conducive to calculation by numerical simulation, following the standard procedure to convert the Hamiltonian into an exactly equivalent Lagrangian. We first express the expectation values and the partition function in terms of an integral over anticommuting fermionic fields, i.e. elements of a Grassmann algebra. (The literature on the path integral formulation of quantum expectation values is very rich. In our work we followed the very clear and useful formulation given in the first chapters of [10].) This gives origin to an integrand with an exponential containing a quadratic form in the fermionic fields, from H_2 and the normal ordering of H_C, as well as a quartic expression, from H_C. The quartic expression can be reduced to a quadratic form by a Hubbard-Stratonovich transformation [11], through the introduction of a suitable auxiliary bosonic field (in our case a real field), and now the Gaussian integral over the fermionic variables can be explicitly performed, leaving an integral over the bosonic field only [12]. The problem, however, is to obtain an integral that can be interpreted as an integration over a well defined probabilistic measure, which can be approximated by stochastic simulation techniques. We show here how the symmetries of the system make this possible.

We start by rewriting the expression for the charge as

$$q_x = a^\dagger_{x,1}a_{x,1} - a_{x,-1}a^\dagger_{x,-1}. \tag{5}$$

We now introduce hole creation and annihilation operators for the electrons with spin -1:

$$b^\dagger_x = a_{x,-1}, \quad b_x = a^\dagger_{x,-1} \tag{6}$$

so that the charge becomes

$$q_x = a^\dagger_x a_x - b^\dagger_x b_x. \tag{7}$$

Note that we dropped the spin indices since from now on $a, a^\dagger$ and $b, b^\dagger$ will always refer to spin 1 and -1, respectively. Finally we change the sign of the $b, b^\dagger$ operators on one of the sublattices. The crucial constraint is that all redefinitions of the operators respect the anticommutator algebra. Because H_2 only couples sites on the two different sublattices, it takes the form

$$H_2 = \sum_{\langle x,y\rangle} -\kappa(a^\dagger_x a_y + b^\dagger_x b_y + \mathrm{h.c.}). \tag{8}$$

We introduce fermionic coherent states

$$\begin{aligned} |\psi,\eta\rangle &= e^{-\sum_x(\psi_x a^\dagger_x + \eta_x b^\dagger_x)}|0\rangle, \\ \langle\psi^*,\eta^*| &= \langle 0|e^{-\sum_x(a_x\psi_x + b_x\eta_x)} \end{aligned} \tag{9}$$

where $\psi_x, \psi^*_x, \eta_x, \eta^*_x$ are anticommuting fermionic variables (elements of a Grassmann algebra).

The path integral formulation is obtained by factoring

$$e^{-\beta H} = e^{-H\,\delta}e^{-H\,\delta}\dots e^{-H\,\delta} \quad (N_t \text{ terms}) \tag{10}$$

with $\delta = \beta/N_t$, and then inserting repeatedly among the factors the resolution of the identity expressed in terms of an integral over the fermionic variables. The trace in Eq. 4 must also be expressed in terms of a similar integral (see e.g. [10] for details). This leads to integrals over fermionic fields $\psi_{x,t}, \psi^*_{x,t}, \eta_{x,t}, \eta^*_{x,t}$ (the index $t = 0, \cdots, N_t - 1$ appears because of the multiple resolutions of the identity and can be thought of as an index labeling Euclidean time), which contain in the integrand expressions of the type

$$\langle\psi^*_{x,t}, \eta^*_{x,t}|e^{-H\,\delta}|\psi_{x,t}, \eta_{x,t}\rangle. \tag{11}$$

The last ingredient is the identity

$$\begin{aligned} &\langle\psi^*_{x,t}, \eta^*_{x,t}|F(a^\dagger_x, b^\dagger_x, a_x, b_x)|\psi_{x,t}, \eta_{x,t}\rangle \\ &\quad = F(\psi^*_{x,t}, \eta^*_{x,t}, \psi_{x,t}, \eta_{x,t})e^{\sum_x(\psi^*_{x,t}\psi_{x,t} + \eta^*_{x,t}\eta_{x,t})} \end{aligned} \tag{12}$$

which is true of any normal ordered function F of the operators $a^\dagger_x, b^\dagger_x, a_x, b_x$.

The Hamiltonian is in fact already in normal order except for the local term $e^2V_{xx}q_xq_x$, which can be written as the sum of two normal-ordered pieces,

$$e^2V_{xx}q_xq_x = e^2V_{xx} : q_xq_x : + e^2V_{xx}(a^\dagger_x a_x + b^\dagger_x b_x). \tag{13}$$

By reassigning the quadratic term in Eq. 13 to H_2, the exponent $-H\,\delta$ in Eq. 11 is normal ordered but the exponential $\exp(-H\,\delta)$ is not. However $\exp(-H\,\delta)$ differs from its normal ordered form by terms $O(\delta^2)$. So, in the limit of $N_t \to \infty$ one may replace the operator expression $\exp(-H\,\delta)$ with an exponential involving the fermionic fields, as follows from Eq. 12. This leads to the following expression for the partition function

$$\begin{aligned} Z = \lim_{N_t\to\infty}\int\prod_m d\psi^*_m d\psi_m d\eta^*_m d\eta_m \\ \times e^{-\sum_{m,n}(\psi^*_m M_{m,n}\psi_n + \eta^*_m M_{m,n}\eta_n)}e^{-\sum_{x,y,t}e^2Q_{x,t}V_{x,y}Q_{y,t}\delta} \end{aligned} \tag{14}$$

where $Q_{x,t} = \psi^*_{x,t}\psi_{x,t} - \eta^*_{x,t}\eta_{x,t}$ and we have used m (and n) as a shorthand for the indices x, t. M is a matrix whose components may be deduced from

$$\sum_{m,n} \psi^*_m M_{m,n} \psi_n = \sum_t \Big[\sum_x \psi^*_{x,t}(\psi_{x,t+1} - \psi_{x,t}) + e^2 V_{xx} \psi^*_{x,t}\psi_{x,t}\,\delta - \kappa \sum_{\langle x,y\rangle} (\psi^*_{x,t}\psi_{y,t} + \psi^*_{y,t}\psi_{x,t})\,\delta \Big] \tag{15}$$

where ψ_{x,N_t} must be identified with $-\psi_{x,0}$.

We now can perform a Hubbard-Stratonovich transformation to express the partition function as a Gaussian integral over c-number real variables $\phi_{x,t}$,

$$Z = \int d\phi d\psi^* d\psi d\eta^* d\eta \times e^{-\phi V^{-1}\phi\delta/4 - \psi^*(M+\imath e\Phi)\psi - \eta^*(M-\imath e\Phi)\eta} \tag{16}$$

where $\Phi_{x,t;y,\tau} = (\phi_{x,t}\delta)\,\delta_{x,y}\delta_{t,\tau}$ is a diagonal matrix.

The Gaussian integration over the anticommuting variables can now be done to obtain

$$Z = \int d\phi e^{-\phi V^{-1}\phi\delta/4} \det(M - \imath e\Phi)\det(M + \imath e\Phi). \tag{17}$$

Because of the identity, $\det(M - \imath e\Phi)\det(M + \imath e\Phi) = \det[(M + \imath e\Phi)^\dagger(M + \imath e\Phi)]$ the measure is positive definite. The down spins are treated as antiparticles (holes) moving backward in time relative to the up spins, exactly canceling the phase for each separately. Correlators for the fermion operators are now obtained by integrating the appropriate matrix elements of $(M \pm \imath e\Phi)^{-1}$ with the measure given by Eq. 17.

Equation 17 is the main result of our work. It establishes the partition function and expectation values as integrals over real variables with a positive definite measure. This is a crucial step for the application of stochastic approximation methods. There remains the problem of sampling the field $\phi_{x,t}$ with a measure which contains the determinant of a large matrix. But, following what is done in lattice gauge theory, this challenge can be overcome through the application of the hybrid Monte Carlo (HMC) technique [9]. In a broad outline, in HMC one first replaces the determinants in Eq. 17 with a Gaussian integral over complex pseudofermionic variables $\zeta_{x,t}$:

$$\det\big[(M + \imath e\Phi)^\dagger(M + \imath e\Phi)\big] = \int d\zeta^* d\zeta e^{-\zeta^*(M+\imath e\Phi)^{\dagger\,-1}(M+\imath e\Phi)^{-1}\zeta}. \tag{18}$$

One then introduces real "momentum variables" $\pi_{x,t}$ conjugate to $\phi_{x,t}$ and inserts in Eq. 18 unity written as a Gaussian integral over π. One finally arrives at

$$Z = \int d\phi d\pi d\zeta^* d\zeta \times e^{-\phi V^{-1}\phi\delta/4 - \zeta^*(M+\imath e\Phi)^{\dagger\,-1}(M+\imath e\Phi)^{-1}\zeta - \pi^2/2}. \tag{19}$$

The idea of HMC is to consider the simultaneous distribution of the variables ϕ, π, ζ and ζ^* determined by the measure in Eq. 19. The phase space of these variables is explored by first extracting the π, ζ and ζ^* according to their Gaussian measure, and then evolving the ϕ and π variables with fixed ζ, ζ^* according to the evolution determined by the Hamiltonian

$$\mathcal{H}(\pi,\phi) = \frac{\pi^2}{2} + \frac{\phi V^{-1}\phi\delta}{4} + \zeta^*(M+\imath e\Phi)^{\dagger\,-1}(M+\imath e\Phi)^{-1}\zeta.$$

Because of Liouville's theorem, the combined motion through phase space produces an ensemble of variables distributed according to the measure in Eq. 19 and, in particular, of fields ϕ distributed according to Eq. 17.

Of course, the discussion above assumes that the Hamiltonian evolution of ϕ and π is exact, which will not be the case with a numerical evolution. The HMC algorithm addresses this shortcoming by: 1) approximating the evolution with a symplectic integrator which is reversible and preserves phase space, 2) performing a Metropolis accept-reject step at the end of the evolution, based on the variation of the value of the Hamiltonian.

Numerical Tests We tested our method on the two-site system obtained by taking $L = 1$, which can be solved exactly. We label the sites $x = 0, 1$. With $\kappa = 1/3$, the Hamiltonian $H = H_2 + H_C$ is now

$$H_2 = -(a^\dagger_1 a_0 + a^\dagger_0 a_1 + b^\dagger_1 b_0 + b^\dagger_0 b_1) + \mu(a^\dagger_x a_x + b^\dagger_x b_x)$$

$$H_C = 2e^2(a^\dagger_0 a_0 - b^\dagger_0 b_0)(a^\dagger_1 a_1 - b^\dagger_1 b_1) + \frac{2e^2}{r_0} a^\dagger_x b^\dagger_x a_x b_x$$

where we have taken $V_{0,1} = V_{1,0} = 1/3$ and a local interaction term $V_{0,0} = V_{1,1} = 1/r_0$. The radius r_0 sets the physical scale in lattice units for localization of the net charge at the carbon atom. It must be restricted to $r_0 < 1$ for stability of the vacuum. Also the normal ordering prescription for $e^2 V_{xx} q_x q_x$ in Eq. 13 adds a new contribution to H_2 in the form of an J_3 "chemical potential" $\mu a^\dagger_{x,s}\sigma_3^{ss'} a_{x,s'}$. It is well known [13, 14] that a J_3 chemical potential μ does not introduce a phase in the measure. At the correct value, $\mu = e^2/r_0$, enforces the exact $SU(2)$ "flavor" symmetry of the tight-binding graphene Hamiltonian. For the two-site system, the spin generators of Eq. 3 become

$$J_+ = J^\dagger_- = (-1)^x a^\dagger_x b^\dagger_x \text{ and } J_3 = [a^\dagger_x a_x + b^\dagger_x b_x]/2 - 1,$$

allowing us to unambiguously classify the 16 states as 5 singlets, 4 doublets and one triplet.

We compared HMC results for expectation values of several products of fermionic operators with the corresponding exact values, finding satisfactory agreement. For example, the correlation function

$$C_a(t) = \langle (a_0 - a_1)(t)\,(a^\dagger_0 - a^\dagger_1)(0)\rangle/2 \tag{20}$$

is illustrated in Fig. 2, which shows HMC results converging to the exact correlators for both the free theory with $e = 0$ and an interacting case with $e = 0.5$.

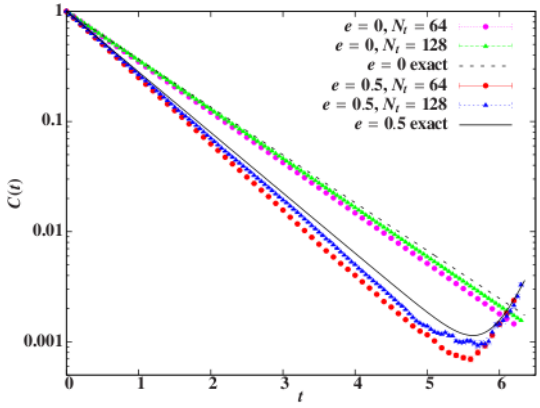

FIG. 2: HMC results for $C_a(t)$ (Eq. 20) with $e = 0$, 0.5 compared to the exact correlators at $r_0 = 1/2$ and $\beta = N_t\delta = 6.4$.

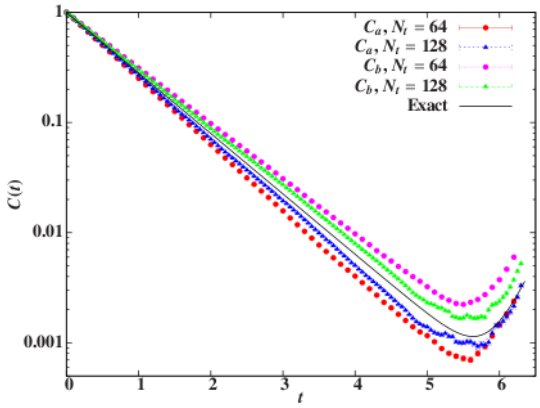

FIG. 3: $C_a(t)$ (Eq. 20) and $C_b(t)$ (Eq. 21) with $e = 0.5$ compared to the exact correlator. Same parameters as in Fig. 2.

A stringent test is to demonstrate the convergence to exact $SU(2)$ symmetry in the "time" continuum limit. To this end, consider a second correlation function,

$$C_b(t) = \langle (b_0^\dagger + b_1^\dagger)(t)\,(b_0 + b_1)(0)\rangle/2\ , \qquad (21)$$

related to $C_a(t)$ by an $SU(2)$ rotation. Fig. 3 illustrates that HMC results for both $C_a(t)$ and $C_b(t)$ converge to the same continuum limit.

We extract the energies of the doublet states at nonzero $\delta = \beta/N_t$ by fitting the correlator data in Fig 3 to single exponentials, $C(t) \approx e^{-Et}$ for fit range $0.4 < t < 4$. The results in Fig. 4 clearly show linear behavior $E \approx E_0 + c_1\delta$, converging to the exact continuum $E_0 = e^2 + \sqrt{4+e^4} - 1 \approx 1.266$. The continuum limit is consistent with restoration of the $SU(2)$ symmetry of the Hamiltonian: a joint linear fit to both sets of energies gives $\lim_{\delta\to 0} E = 1.262 \pm 0.004$, with $c_1 = 1.25 \pm 0.07$ and -0.98 ± 0.04 for correlators C_a and C_b, respectively.

Conclusion We emphasize by taking the time continuum limit of Eq. 16 that our approach has constructed

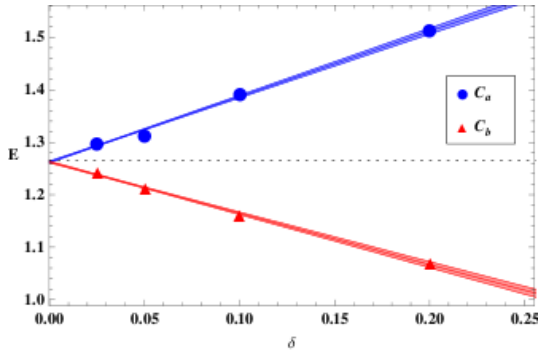

FIG. 4: Linear extrapolation (with error band) of the HMC energies for doublet correlators C_a and C_b as a function of the "time" lattice spacing $\delta = 6.4/N_t$ for $N_t = 32$, 64, 128 and 256. The dotted horizontal line marks $E_0 = 1.266$.

the exact Lagrangian for the tight binding model,

$$\mathcal{L}(t) = \psi_x^\dagger(t)(\partial_t + ie\sigma_3\phi_x(t))\psi_x(t) + e^2 V_{xx}\psi_x^\dagger(t)\psi_x(t) - \kappa\sum_{\langle x,y\rangle}\psi_x^\dagger(t)\psi_y(t) + \frac{1}{4}\phi_x(t)V_{xy}^{-1}\phi_y(t)\ , \qquad (22)$$

where we have defined two component spinor fields, $(\psi_{x,t}^*, \eta_x^*) \to \psi_x^\dagger(t)$ and $(\psi_{x,t}, \eta_x)^T \to \psi_{x,t}(t)$, in the continuum. The exact two site solution supports this claim.

Introducing a discrete Euclidean time does not have a sign problem if we restrict the hopping term to nearest neighbor lattice sites. We anticipate that the phenomenological next-to-nearest neighbor coupling $\kappa'/\kappa \simeq 0.05$ can be accommodated by reweighting without a prohibitive cost. Our method enables accurate prediction of the tight binding theory for graphene utilizing the full arsenal of computational physics introduced by lattice field theorists in particle and condensed matter physics. This opens up a range of new numerical studies of phenomena relevant to experimental investigations of graphene, such as those due to finite lattice deformations, interaction with phonons and external electromagnetic fields. Our first objective [15] is to accurately determine the critical charge for the semimetal-insulator transition for a single layer graphene in the tight binding theory and then to explore how changing the environment might alter the transition to allow it to switch phases.

Acknowledgments: We wish to acknowledge the many fruitful conversations with Dr. Ronald Babich, Prof. Antonio Castro Neto and Prof. Claudio Chamon during the course of this research and support under DOE grants DE-FG02-91ER40676, DE-FC02-06ER41440, and NSF grants OCI-0749317, OCI-0749202. Part of this work was completed while two of the authors were at the Aspen Center for Physics.

[1] K. S. Novoselov, A. K. Geim, S. V. Morozov, D. Jiang, Y. Zhang, S. V. Dubonos, I. V. Grigorieva and A. A. Firsov "Electric Field Effect in Atomically Thin Carbon Films", *Science* **306**, 666 (2004).

[2] A. K. Geim and K. S. Novoselov, "The rise of graphene", *Nature Mat.* **6**, 183 (2007).

[3] A. H. Castro Neto, F. Guinea, N. M. R. Peres, K. S. Novoselov and A. K. Geim, "The electronic properties of graphene", *Rev. Mod. Phys.* **81**, 109 (2009).

[4] H. J. Rothe, *Lattice Gauge Theories: An Introduction*, (World Scientific, Singapore, 2005).

[5] J. E. Drut and T. A. Lähde, "Is Graphene in Vacuum an Insulator?", *Phys. Rev. Lett.* **102**, 026802 (2009).

[6] J. E. Drut and T. A. Lähde, "Lattice field theory simulations of graphene", *Phys. Rev. B* **79**, 165425 (2009).

[7] Wesley Armour, Simon Hands and Costas Strouthos, "Monte Carlo simulation of monolayer graphene at nonzero temperature", *Phys. Rev. B* **84**, 075123 (2011).

[8] Timo A. Lähde and Joaquín E. Drut, "Strongly coupled Graphene on the Lattice", *Proc. Sci.* **Lattice 2011**, 074 (2011).

[9] Simon Duane, A. D. Kennedy, Brian J. Pendleton and Duncan Roweth, "Hybrid Monte Carlo" *Phys. Lett. B* **195**, 216 (1987).

[10] J. W. Negele and H. Orland, *Quantum Many Particle Systems*, (Addison-Wesley, Redwood City, California, 1988).

[11] R. L. Stratonovich, "On a Method of Calculating Quantum Distribution Functions", *Sov. Phys. Dokl.* **2**, 416 (1958); J. Hubbard, "Calculation of Partition Functions", *Phys. Rev. Lett.* **3**, 77 (1959).

[12] R. Blankenbecler, D. J. Scalapino and R. L. Sugar, Monte Carlo calculations of coupled boson-fermion systems. I *Phys. Rev. D* **24**, 2278 (1981).

[13] M. G. Alford, A. Kapustin and F. Wilczek, "Imaginary chemical potential and finite fermion density on the lattice", *Phys. Rev. D* **59**, 054502 (1999).

[14] D. T. Son and M. A. Stephanov, "QCD at finite isospin density", *Phys. Rev. Lett.* **86**, 592 (2001).

[15] Richard Brower, Claudio Rebbi and David Schaich, "Hybrid Monte Carlo simulation on the graphene hexagonal lattice", *Proc. Sci.* **Lattice 2011**, 056 (2011).